Chemistry of Metals and Alloys

Chem. Met. Alloys 12 (2019) 44-49
Ivan Franko National University of Lviv
www.chemetal-journal.org

Influence of Ho substitution on the structural and magnetic properties of $DyCu_5Sn$

A. ZELINSKIY[1], M. BOBNAR[2], O. SICHEVYCH[2], L. AKSELRUD[1,2], L. ROMAKA[1], R. GLADYSHEVSKII[1]

[1] *Department of Inorganic Chemistry, Ivan Franko National University of Lviv, Kyryla i Mefodiya St. 6, 79005 Lviv, Ukraine*
[2] *Max-Planck-Institut für Chemische Physik fester Stoffe, Nöthnitzer Straße 40, 01187 Dresden, Germany*
* *Corresponding author. Tel.: +380-32-2600388; e-mail: anatoliy.zelinskiy@gmail.com*

Received May 12, 2019; accepted June 18, 2019; available on-line January 1, 2020
https://doi.org/10.30970/cma12.0394

Several samples from the homogeneity range of the solid solution $Dy_{1-x}Ho_xCu_5Sn$ (x = 0-0.1) were prepared by arc melting of the elements and annealed first at 1100 K and then at 870 K. The crystal structure of $DyCu_5Sn$ was solved from single-crystal *X*-ray diffraction data, and Rietveld refinements of *X*-ray powder diffraction data were carried out to analyze the evolution of the lattice parameters in the solid solution. The $Dy_{1-x}Ho_xCu_5Sn$ phase crystallizes with the structure type $CeCu_5Au$ (an ordered variant of the $CeCu_6$ type). The replacement of Dy by Ho is accompanied by a decrease of the volume of the unit cell. The magnetic behavior of the $Dy_{1-x}Ho_xCu_5Sn$ intermetallics was studied by magnetic susceptibility (χ) measurements in the temperature range 1.8-400 K. Contrary to earlier reports a paramagnetic Curie temperature of -3.9 K was found for $DyCu_5Sn$, but the magnetic behavior of the sample $Dy_{0.9}Ho_{0.1}Cu_5Sn$, with a critical temperature near 0 K, can be described by a quantum phase transition associated with an antiferromagnetic transformation.

Intermetallics / Crystal structure / X-ray diffraction / Magnetic properties / Quantum phase transition

Introduction

Two series of ternary compounds with high Cu content have been reported in most of the rare earth–copper–tin systems, *i.e.* $R_{1.9}Cu_{9.2}Sn_{2.8}$ (R = Y, Ce-Sm, Gd-Lu) with a hexagonal structure related to the $CeNi_5Sn$ type [1], and RCu_5Sn ($CeCu_6$-type structure), which forms with all rare earths except Lu [2,3]. Another study of the RCu_5Sn stannides with R = La-Gd [4] by the single-crystal method showed crystal structures corresponding to the $CeCu_5Au$ type (ordered variant of the $CeCu_6$ type) [5]. The structures of both series, $R_{1.9}Cu_{9.2}Sn_{2.8}$ and RCu_5Sn, are related to the binary $CaCu_5$ type.

Among the RCu_5Sn stannides with light rare earths, magnetic properties have been studied for $CeCu_5Sn$ and $PrCu_5Sn$ [2,4]. $CeCu_5Sn$ orders antiferromagnetically, while $PrCu_5Sn$ is in a non-magnetic ground state. Studies of the magnetic properties of the RCu_5Sn series of intermetallics where R = Gd-Yb, in the temperature range from 2 to 300 K [3], indicated that the stannides with Gd, Tb, Dy, Ho, and Er order antiferromagnetically at low temperature. In contrast, $TmCu_5Sn$ and $YbCu_5Sn$ do not exhibit magnetic ordering down to 2 K.

Electrical resistivity data indicated metallic type of conductivity for all the studied stannides where R is Y, Gd-Tm [6]. The magnetic ordering observed earlier for the $GdCu_5Sn$, $TbCu_5Sn$, and $DyCu_5Sn$ compounds was confirmed by electrical resistivity measurements.

It is worth noting that in [3] the paramagnetic Curie temperature θ_p of $DyCu_5Sn$ was found to be equal to 0 K ("ideal" paramagnetism). Such compounds can be potential candidates for the search for new quantum materials, because the properties of these systems are uniquely defined by quantum mechanical effects. Taking into account the literature data we decided to investigate the structural and magnetic characteristics of $DyCu_5Sn$ modified by Ho. The aim of the present work was the detailed investigation of the solid solution $Dy_{1-x}Ho_xCu_5Sn$ (x = 0-0.1).

Experimental details

Alloys were prepared by weighing appropriate amounts of Dy and Ho metals (purity 99.9 wt.%), Cu metal (purity 99.99 wt.%), and Sn metal (purity

99.999 wt.%). The charges were arc-melted under purified, Ti-gettered, argon atmosphere, using a non-consumable tungsten electrode and a water-cooled copper hearth. The ingots were sealed in Ta tubes and annealed in evacuated silica ampoules first at 1100 K for 120 h and then at 870 K for 720 h, and subsequently quenched in ice water.

Phase identification and refinement of the lattice parameters were performed on room-temperature powder X-ray diffraction data (image-plate Guinier camera Huber G670, Cu $K\alpha_1$ radiation, λ = 1.5405 Å), using LaB_6 as internal standard (a = 4.15692 Å).

The crystal structure of $DyCu_5Sn$ was determined on an irregularly shaped single crystal isolated from a centrifuged sample, the quality of which had preliminarily been checked by Laue photographs. The intensity data collection was performed on a Rigaku AFC7 diffraction system equipped with a Mercury CCD detector using Mo $K\alpha$ radiation (λ = 0.71073 Å). A numerical absorption correction of the reflection intensities was performed based on an optimized description of the crystal faces [7].

The WinCSD program package [8] was used for crystal structure solution and refinement, for single-crystal and powder diffraction data.

Magnetic susceptibility measurements were carried out in magnetic fields of up to 70 kOe in the temperature range from 1.8 to 400 K, using a magnetometer MPMS 3, Quantum Design on multicrystal agglomerates.

A cross section (0.5×0.5 mm^2) of an annealed sample was prepared by grinding (SiC) and diamond polishing using alcohol-based lubricants suitable for water-sensitive materials. Light optical (Zeiss Axioplan 2) and scanning electron microscopy (SEM, Philips XL30) images were taken. The local chemical composition of the samples was determined by semiquantitative energy-dispersive X-ray spectroscopy using an EDX system (Bruker, Quantax 400) attached to the SEM. An $\Phi(\rho z)$ matrix correction was applied to calculate the local mass concentrations from the measured X-ray intensities. Final atomic concentrations were evaluated after normalizing and averaging on three measurements.

Results and discussion

Crystal structure

The microstructure of the sample with nominal composition $Dy_{14.3}Cu_{71.4}Sn_{14.3}$ was mainly formed by the target phase $DyCu_5Sn$ (Fig. 1). The EDX spectra solely showed the presence of the expected elements. The composition of the majority phase as obtained by EDX, $Dy_{14.28(2)}Cu_{71.41(3)}Sn_{14.31(2)}$ (uncertainties were calculated from three measured points), agrees well with $Dy_{14.3}Cu_{71.4}Sn_{14.3}$, obtained from the crystal structure determination. Traces of tin metal were observed on the grain boundaries of the majority phase.

Analysis of single-crystal X-ray diffraction data for $DyCu_5Sn$ indexed on an orthorhombic lattice (a = 8.20467(9), b = 4.96952(5), c = 10.5733(1) Å, from powder X-ray data with LaB_6 as internal standard) led to the possible space groups $Pn2_1a$ and $Pnma$. The structure was solved in the centrosymmetric space group $Pnma$ by application of direct methods.

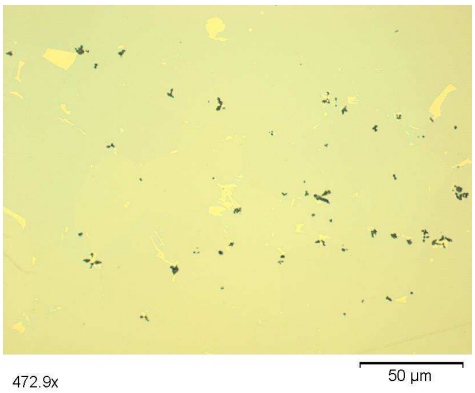

Fig. 1 Microstructure of the sample $Dy_{14.3}Cu_{71.4}Sn_{14.3}$.

Crystallographic information and details of the data collection are given in Table 1. Atomic coordinates and displacement parameters for $DyCu_5Sn$ are presented in Table 2 and Table 3. The interatomic distances within the coordination polyhedra are listed in Table 4.

The coordination polyhedra of the atoms in the structure of $DyCu_5Sn$ are shown in Fig. 2.

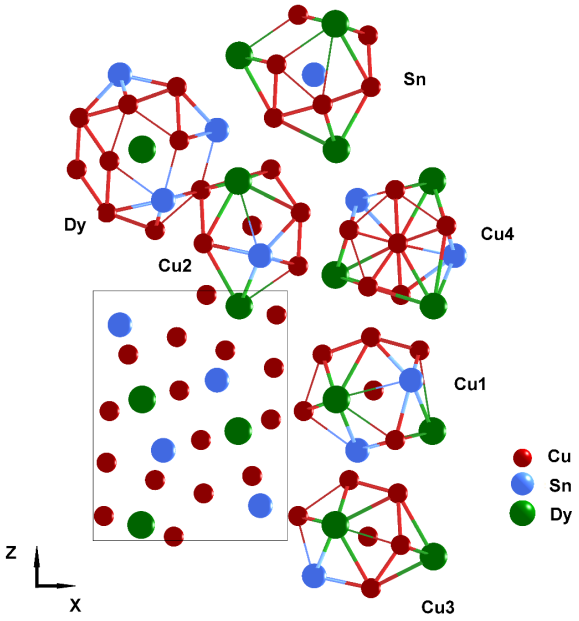

Fig. 2 Projection of the structure of $DyCu_5Sn$ onto the XZ plane and coordination polyhedra of the different atoms.

Distorted pseudo Frank-Kasper 19-vertex polyhedra can be considered for the Dy atoms [$Cu_{15}Sn_4$] and 14-vertex Frank-Kasper polyhedra for the Sn atoms [$Cu_{10}Dy_4$]. The Cu1 atoms are surrounded by 13-vertex polyhedra [$Cu_7Sn_3Dy_3$]. The Cu2, Cu3, Cu4 atoms are located at the centers of distorted icosahedra: [$Cu_7Sn_2Dy_3$] for the Cu2 and Cu4 atoms, [Cu_8SnDy_3] for the Cu3 atoms.

Previous structure refinements [3,9] with R = Gd and Er showed a small deviation from the 1:5:1 stoichiometry, giving a composition $RCu_{5-x}Sn_{1+x}$. According to the refinements performed in this work, the $DyCu_5Sn$ with $CeCu_5Au$-type structure is characterized by an ordered distribution of the atoms, which corresponds to the formula RCu_5Sn.

The crystal structure of the solid solution $Dy_{1-x}Ho_xCu_5Sn$ was refined on X-ray powder diffraction data. According to the refinements this solid solution crystallizes with the same $CeCu_5Au$ type. The lattice parameters refined on samples within the homogeneity range are listed in Table 5. Observed, calculated and difference X-ray patterns of the $(Dy_{0.9}Ho_{0.1})Cu_5Sn$ sample are shown in Fig. 3.

Table 1 Crystal data and details of the data collection for single-crystal $DyCu_5Sn$.

Composition	$DyCu_5Sn$
Space group	*Pnma* #62
Pearson symbol	*oP*28
Formula units per unit cell, Z	4
Lattice parameters [a] a, b, c (Å); V (Å)^3	8.20467(9), 4.96952(5), 10.5733(1); 431.11(1)
Diffraction system	RIGAKU AFC7
Detector	Mercury CCD
Radiation, λ (Å)	Mo $K\alpha$, 0.71073
Scan; step (degree); N (images)	φ, 0.6, 600
Maximum 2θ (degree)	85.97
Range in h, k, l	$-11 \le h \le 15$, $-5 \le k \le 9$, $-20 \le l \le 16$
Absorption correction	numerical
T_{max}-T_{min}	1.0-0.38
Absorption coefficient (1/cm)	483.63
Mode of refinement	$F(hkl)$
Observation criteria	$F(hkl) > 4\sigma(F)$
Number of measured reflections	8361
Number of independent reflections	1540
Refined parameters	40
Reliability factors R_F, R_w; Goodness of fit S	0.0319, 0.0331; 1.04
Residual peaks (e/Å^3)	-2.17/3.21

[a] X-ray powder diffraction data (camera Huber G670, Cu $K\alpha_1$ radiation, LaB_6 as internal standard, a = 4.15692 Å)

Table 2 Atom coordinates and site occupancies for $DyCu_5Sn$.

Atom	Wyckoff position	*x*/*a*	*y*/*b*	*z*/*c*	Occupancy
Dy	4*c*	0.25237(6)	¼	0.5628(5)	1
Cu1	4*c*	0.0574(2)	¼	0.1002(2)	1
Cu2	4*c*	0.3169(2)	¼	0.2419(2)	1
Cu3	4*c*	0.4153(2)	¼	0.0165(1)	1
Cu4	8*d*	0.0699(1)	0.5011(1)	0.31142(8)	1
Sn	4*c*	0.13829(8)	¼	0.86052(6)	1

Table 3 Equivalent and anisotropic displacement parameters (Å^2) for $DyCu_5Sn$.

Atom	B_{eq}	B_{11}	B_{22}	B_{33}	B_{12}	B_{13}	B_{23}
Dy	0.81(1)	0.66(1)	0.93(2)	0.84(2)	0	0.03(1)	0
Cu1	0.95(2)	0.83(4)	1.41(5)	0.59(3)	0	0.05(3)	0
Cu2	0.85(2)	0.54(3)	1.14(4)	0.88(4)	0	0.11(3)	0
Cu3	0.86(2)	0.98(4)	1.06(4)	0.55(3)	0	-0.06(3)	0
Cu4	0.75(2)	0.68(2)	0.79(3)	0.77(2)	-0.05(2)	0.03(2)	-0.08(2)
Sn	0.69(1)	0.55(2)	0.93(2)	0.59(2)	0	0.01(2)	0

Table 4 Interatomic distances in the structure of $DyCu_5Sn$.

Atoms		δ, Å	Atoms		δ, Å	Atoms		δ, Å
Dy	-2 Cu3	2.882(1)	Cu2	-2 Cu4	2.487(2)	Cu4	-1 Cu4	2.474(1)
	-1 Cu3	2.890(2)		-2 Cu4	2.491(2)		-1 Cu2	2.487(2)
	-2 Cu1	2.961(1)		-1 Cu3	2.517(2)		-1 Cu2	2.491(2)
	-1 Cu1	3.038(2)		-1 Cu1	2.585(2)		-1 Cu4	2.496(1)
	-2 Cu2	3.176(1)		-1 Cu1	2.604(2)		-1 Cu3	2.499(2)
	-2 Cu4	3.208(1)		-2 Sn	2.8074(8)		-1 Cu3	2.545(2)
	-2 Cu4	3.251(1)		-2 Dy	3.176(1)		-1 Cu1	2.561(2)
	-1 Sn	3.268(1)		-1 Dy	3.434(2)		-1 Sn	2.745(1)
	-1 Sn	3.283(1)	Cu3	-2 Cu4	2.499(2)		-1 Sn	2.784(1)
	-2 Cu4	3.296(1)		-1 Cu2	2.517(2)		-1 Dy	3.208(1)
	-2 Sn	3.399(1)		-2 Cu4	2.545(2)		-1 Dy	3.251(1)
	-1 Cu2	3.434(2)		-1 Sn	2.808(2)		-1 Dy	3.296(1)
Cu1	-2 Cu4	2.561(2)		-2 Cu3	2.868(1)	Sn	-1 Cu1	2.619(2)
	-1 Cu2	2.585(2)		-2 Dy	2.882(1)		-2 Cu4	2.745(1)
	-1 Cu2	2.604(2)		-1 Dy	2.890(2)		-2 Cu4	2.784(1)
	-1 Sn	2.619(2)		-1 Cu1	3.068(2)		-2 Cu2	2.807(1)
	-2 Dy	2.961(1)					-1 Cu3	2.808(2)
	-2 Sn	2.987(1)					-2 Cu1	2.987(1)
	-1 Dy	3.038(2)					-1 Dy	3.268(1)
	-1 Cu3	3.068(2)					-1 Dy	3.284(1)
	-2Cu1	3.398(1)					-2 Dy	3.399(1)

Table 5 Lattice parameters and paramagnetic Curie temperature for the solid solution $Dy_{1-x}Ho_xCu_5Sn$.

Composition	a (Å)	b (Å)	c (Å)	V (Å^3)	θ_p (K)
$DyCu_5Sn$	8.20467(9)	4.96952(5)	10.5733(1)	431.11(1)	-3.93
$Dy_{0.96}Ho_{0.04}Cu_5Sn$	8.20425(7)	4.96883(4)	10.5728(1)	431.02(1)	-11.74
$Dy_{0.94}Ho_{0.06}Cu_5Sn$	8.20352(9)	4.96876(5)	10.5728(1)	430.96(2)	-6.91
$Dy_{0.90}Ho_{0.10}Cu_5Sn$	8.20320(7)	4.96824(4)	10.5725(1)	430.89(1)	0.01

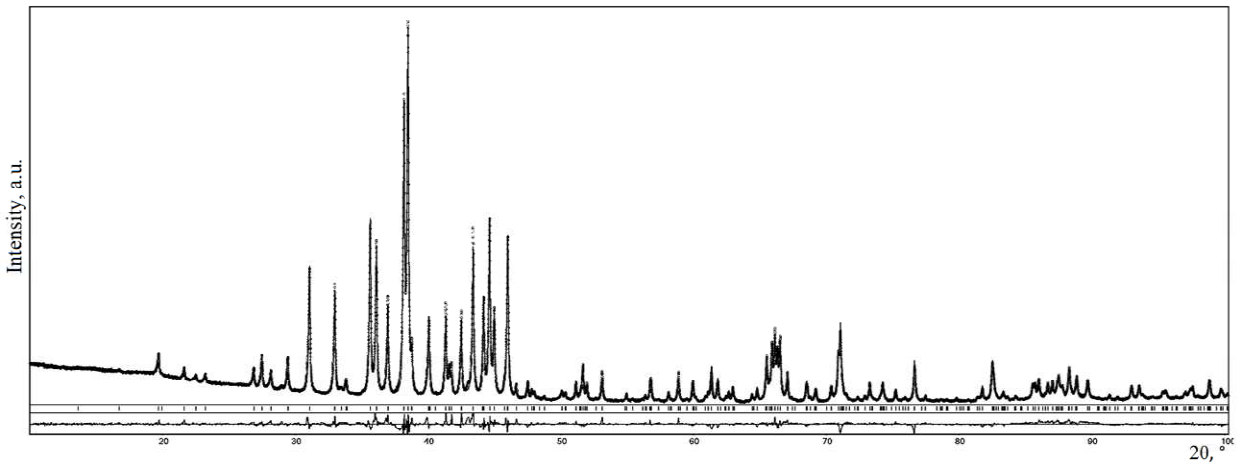

Fig. 3 Observed, calculated and difference (bottom) X-ray diffraction powder patterns of $(Dy_{0.9}Ho_{0.1})Cu_5Sn$.

Magnetic properties

The magnetic behavior of the $DyCu_5Sn$ and $Dy_{1-x}Ho_xCu_5Sn$ intermetallics was studied by magnetic susceptibility (χ) measurements in the temperature range 1.8-400 K in a static magnetic field. From the $1/\chi(T)$ dependence the paramagnetic Curie temperature θ_p was determined and the effective magnetic moment μ_{eff} was calculated. The temperature dependence of the inverse magnetic susceptibility for the $DyCu_5Sn$ compound is shown in Fig. 4. In the paramagnetic region, the magnetic susceptibility follows the Curie-Weiss law and only the Dy^{3+} ions determine the

magnetic behavior. The calculated effective magnetic moment per formula unit is close to the value of the free Dy^{+3} ion (Table 6). A pronounced maximum characteristic of antiferromagnetic ordering is observed at T_N = 13 K.

Table 6 Magnetic characteristics of the $DyCu_5Sn$ compound.

T_N (K)	θ_p (K)	μ_{eff} (μ_B)		Ref.
		exp.	calc.	
-13	-3.93	10.60(1)	10.65	this work
-13.0	0	10.90		[3]

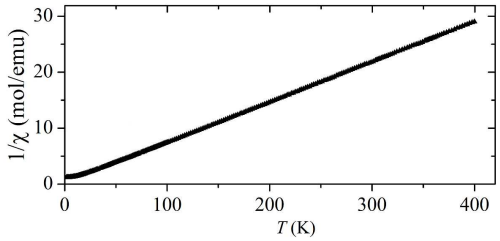

Fig. 4 Temperature dependence of the inverse magnetic susceptibility of $DyCu_5Sn$.

The field dependence of the magnetization up to 70 kOe at 1.8 K for $DyCu_5Sn$ (Fig. 5) showed that magnetic saturation is not reached in the maximum applied field. Below T_N the compound exhibits a metamagnetic transition with a critical field of about 12 kOe, which correlates with antiferromagnetic ordering.

The temperature dependence of the inverse magnetic susceptibility for the $Dy_{0.9}Ho_{0.1}Cu_5Sn$ sample is presented in Fig. 6b. The composition dependencies of the paramagnetic Curie temperature and the unit-cell volume are presented in Fig. 6a, and the values of the lattice parameters and the paramagnetic Curie temperature for the $Dy_{1-x}Ho_xCu_5Sn$ samples are listed in Table 5.

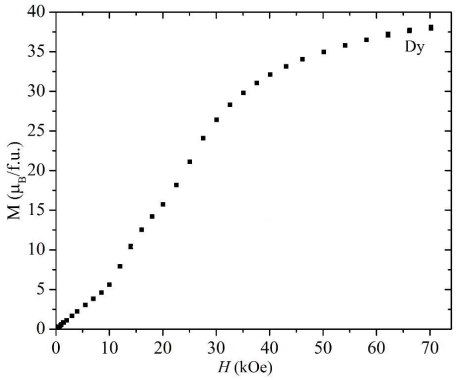

Fig. 5 Magnetization *versus* applied field at 1.8 K for $DyCu_5Sn$.

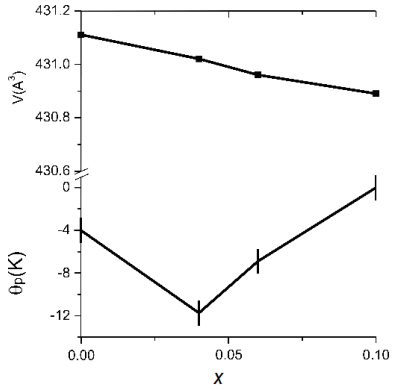

a

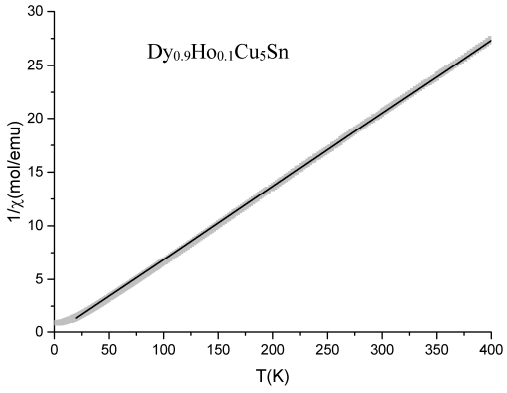

b

Fig. 6 Composition dependence of the paramagnetic Curie temperature and unit-cell volume of $Dy_{1-x}Ho_xCu_5Sn$ (*a*) and temperature dependence of the inverse magnetic susceptibility of $Dy_{0.9}Ho_{0.1}Cu_5Sn$ (*b*).

Conclusions

The crystal structure of the ternary compound $DyCu_5Sn$ was studied by single-crystal X-ray diffraction and the crystal structure of the solid solution $Dy_{1-x}Ho_xCu_5Sn$ by X-ray powder diffraction. The analysis of the crystal structure confirmed the ordered $CeCu_5Au$ type for $DyCu_5Sn$.

The magnetic measurements performed in our work confirmed antiferromagnetic ordering at T_N = 13 K for the compound $DyCu_5Sn$. However, in contrast to the conclusions drawn in [3], the value of the paramagnetic Curie temperature, θ_p = -3.93 K, differed significantly from 0 K. The value of the effective magnetic moment μ_{eff} = 10.60 μ_B calculated from the temperature dependence of the magnetic

susceptibility is in good agreement with the theoretical value for the free Dy^{3+} ion. The value of μ_{eff} reported for the same compound in [3] was slightly higher (10.90 μ_B).

The replacement of Dy by Ho in the $CeCu_5Au$-type structure is accompanied by a decrease of the unit-cell volume. The magnetic behavior of the sample $Dy_{0.9}Ho_{0.1}Cu_5Sn$, with a critical temperature of about 0 K can be described by a quantum phase transition associated with an antiferromagnetic transformation.

Acknowledgments

The authors are grateful to Dr. U. Burkhardt, P. Scheppan and M. Eckert for EDX and S. Hückmann for the powder X-ray diffraction measurements.

References

[1] V.V. Romaka, D. Fruchart, R. Gladyshevskii, P. Rogl, N. Koblyuk, *J. Alloys Compd.* 460 (2008) 283-288.

[2] R.V. Skolozdra, L.P. Romaka, L.G. Akselrud, J. Pierre, *J. Alloys Compd.* 262-263 (1997) 346-349.

[3] Ya. Mudryk, O. Isnard, L. Romaka, D. Fruchart, *Solid State Commun.* 119 (2001) 423-427.

[4] M.L. Fornasini, R. Marazza, D. Mazzone, P. Riani, P. Zanicchi, *Z. Kristallogr.* 213 (1998) 108-111.

[5] M. Ruck, G. Portisch, H.G. Schlager, M. Sieck, H.V. Lohneysen, *Acta Crystallogr. B* 49 (1993) 936-941.

[6] I. Romaniv, L. Romaka, B. Kuzhel, V.V. Romaka, M. Rudchenko, Yu. Stadnyk, M. Konyk, M. Rudko, *Chem. Met. Alloys* 12 (2019) 1-8.

[7] X-SHAPE, Version 1.06, *Crystal Optimisation for Numerical Absorption Correction*; Darmstadt, Germany, 1999.

[8] L. Akselrud, Yu. Grin, *J.Appl. Crystallogr.* 47 (2014) 803-805.

[9] L. Romaka, V.V. Romaka, E.K. Hlil, D. Fruchart, *Chem. Met. Alloys* 2 (2009) 68-74.